Mineralogical Magazine, December 1999, Vol. 63(6), pp. 917–926

Disorder and compositional variation in the lillianite homologous series

A. PRING[1], M. JERCHER[1,*] AND E. MAKOVICKY[2]

[1] Department of Mineralogy, South Australian Museum, North Terrace, Adelaide, South Australia 5000, Australia
[2] Mineralogical Institute, University of Copenhagen, Øster Voldgade 5–7, DK-1350 Copenhagen, Denmark

ABSTRACT

High resolution transmission electron microscopy studies on the lillianite group minerals from the Ivigtut cryolite deposit, Ivigtut, South Greenland revealed the existence of disordered intergrowths of lillianite/gustavite-like blocks ($N = 4$) and heyrovskyite-like ($N = 7$) structural blocks. One disorder sequence is examined in detail, which gave an average homologue number $N = 4.92$ corresponding to a composition of $Pb_{3.92-2x}Bi_{2-x}Ag_xS_{6.92}$ with $x \approx 1.2$. An Axial Next-Nearest Neighbour Ising model was used to follow the fluctuations in the average homologue number N across the crystal. This yielded compositional fluctuations of the order of 70–170 Å over a 1800 Å region of the crystal, with a 202 Å lamella of ordered vikingite. Trends in the randomness of the gustavite-vikingite intergrowth were evaluated and the dominant slab sequence was found to be 4,4,4,7 and 4,4,7,7, suggesting that some longer period homologues may be stable. A number of defects were noted in which changes in slab widths were accommodated. The origin of these partially ordered/disordered lillianite homologues is discussed.

KEYWORDS: lillianite group minerals, disorder, HRTEM, Ivigtut, Greenland.

Introduction

THE development of structural classification systems in which complex structures are reduced to a set of simple fundamental blocks and a set of building or assembly instructions has done much to emphasize and simplify the relationships between minerals within a given group. Our understanding of the chemistry, structure and paragenesis of the sulphosalt minerals has benefited by such systematic treatments. This is particularly so for the Pb sulphosalts that can be related to PbS and SnS parent structures (Makovicky, 1981, 1985, 1989). High-resolution transmission electron microscopy (HRTEM) studies of a number of mineral systems, notably the biopyriboles and the humites, have revealed the existence of disordered intergrowths of structural blocks of varying sizes. The disordered intergrowth of different blocks provides a mechanism for compositional variation in these systems (Veblen *et al.*, 1977, Veblen and Buseck, 1979; White and Hyde, 1982*a,b*). Disordered intergrowths of compositionally distinct but structurally similar slabs have been shown to account for compositional fields in the bismuthinite-aikinite series (Pring, 1989, 1995).

Defect structures and disordered intergrowths have been reported from studies on synthetic members of the lillianite group Pb–Bi(Ag)–S (Skowron and Tilley, 1986, 1990; Tilley and Wright, 1982), but to date such phenomena have not been confirmed in natural lillianites. Makovicky and Karup-Møller (1977*b*) documented evidence of disorder in 'single crystal' X-ray diffraction patterns of lillianites from the gustavite-cosalite-galena paragenesis from the Ivigtut cryolite deposit, Ivigtut, South Greenland (Karup-Møller 1977). Here we report the preliminary results of a HRTEM study on some lillianite group minerals from the Ivigtut cryolite deposit.

* Current address: Anger Straße 27, 40593 Düsseldorf, Germany.

The lillianite group

The lillianite homologous series is a group of Pb–Bi(Ag) sulphosalts that have structures based on the ordered intergrowth of slabs of 'galena-like' structure cut parallel to $(311)_{PbS}$. The blocks have a 'chemically twinned' arrangement and the overlapping MS_6 octahedra of the adjacent, mirror-related units are substituted by bi-capped trigonal prisms (PbS_{6+2}) (Fig. 1) (Makovicky, 1977; Makovicky and Karup-Møller, 1977*a,b*).

Distinct homologues in the series differ in the width of the galena-like slabs. This can conveniently be expressed by N, the number of metal sites in the chains of octahedra, which run diagonally across individual galena-like slabs and parallel to $[011]_{PbS}$. Homologues are denoted ^{N1,N2}L, where $N1$ and $N2$ are the number of metal sites in the two alternating slabs and the chemical composition is constrained by the formula

$$Pb_{N-1-2x}Bi_{2+x}Ag_xS_{N+2}$$

where $\mathbf{N} = (N1+N2)/2$ and x is the Ag+Bi = 2Pb substitution coefficient with $x_{max} = (\mathbf{N}-2)/2$. All homologues reported to date conform to this formula and it is important to note that the individual homologue slabs are electrostatically neutral.

Only two Ag-free lillianite homologues are known in nature, lillianite, $Pb_3Bi_2S_6$ (^{4,4}L) and heyrovskyite, $Pb_6Bi_2S_9$ (^{7,7}L) (however, they both usually contain a small amount of Ag). In the Pb–Bi–Ag–S system, several more orthorhombic ($N1=N2$) and monoclinic ($N1 \neq N2$) members exist, including gustavite, (^{4,4}L) and vikingite, (^{4,7}L) (Table 1). Complete solid solution between lillianite and gustavite has been shown to exist above 500°C in synthetic studies (Hoda and Chang, 1975); however, there are apparent miscibility gaps in the 'gustavite solution' when formed under natural hydrothermal conditions (Makovicky and Karup-Møller, 1977*b*). The end-members are gustavite, $PbAgBi_3S_6$ and lillianite $Pb_3Bi_2S_6$ and intermediate compositions can be expressed in terms of % of the end member, $Pb_2Ag_{0.5}Bi_{2.5}S_6$ being the mid-member (Gus_{50} still in the lillianite composition field). Vikingite compositions can also be expressed in terms of a hypothetical series between $Pb_4Ag_7Bi_{15}S_{30}$ (Vik_{100}) and $Pb_{18}Bi_8S_{30}$ (Vik_0), with the composition of vikingite from Ivigtut being between 67–73% Ag–Bi substitution (Makovicky and Karup-Møller, 1977*b*). Chemical analyses of many lillianite homologues give non-integral values for N, and Makovicky (1981) suggested that the differences may either be due to analytical problems or to errors in the frequency of the 'chemical twinning' (i.e. block-width disorder). Streaking on single crystal X-ray diffraction photographs of higher homologues

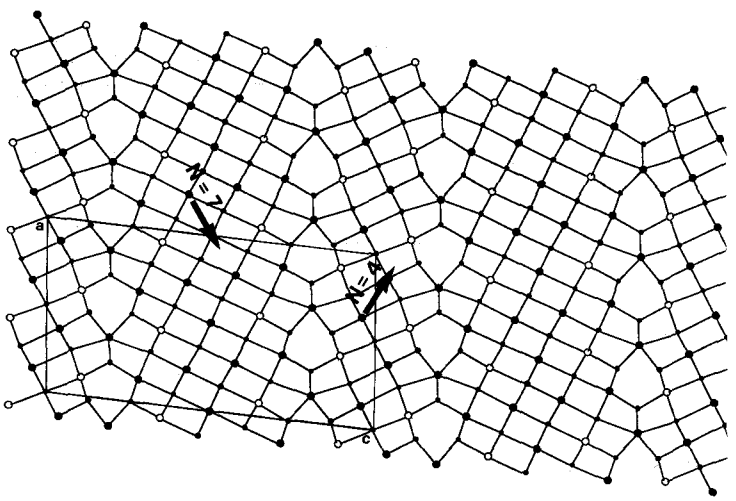

FIG. 1. Structural diagram of vikingite showing the atomic arrangement in the ^{4}L and ^{7}L units. The larger circles represent Pb(Ag) filled, and Bi(Ag) open; the small circles represent S. Arrows indicate directions of $[011]_{PbS}$ chains of octahedra.

TABLE 1. Summary of compositional and structural data for the members of the lillianite homologous series (after Makovicky, 1981)

Mineral	Formula	Structure	Cell repeats			Angle	Space group	Diagnostic reflection
Lillianite	$Pb_3Bi_2S_6$	$^{4,4}L$	*a*13.54	*b*20.45	*c*4.10	–	*Bbmm*	0 12 0
Gustavite	$PbAgBi_3S_6$	$^{4,4}L$	*a*7.08	*b*19.57	*c*8.27	β107.2	$P2_1/c$	0 12 0
Vikingite	$Pb_8Ag_5Bi_{13}S_{30}$	$^{4,7}L$	*a*13.60	*c*25.25	*b*8.22	β95.6	*P2/a*	0 0 15
Treasurite	$Pb_6Ag_7Bi_{15}S_{32}$	$^{4,8}L$	*a*13.35	*c*26.54	*b*4.09	β92.8	*C2/m*	0 0 16
Heyrovskyite	$Pb_6Bi_2S_9$	$^{7,7}L$	*a*13.71	*b*31.21	*c*4.13	–	*Bbmm*	018 0
Eskimoite	$Pb_{10}Ag_7Bi_{15}S_{36}$	$^{5,9}L$	*b*13.46	*c*30.18	*b*4.10	β93.4	*C2/m*	0 0 18
Ourayite	$Pb_{15}Ag_{12.5}Bi_{20.5}S_{52}$	$^{11,11}L$	*b*13.46	*c*26.54	*b*4.09	β92.8	*C2/m*	0 0 26
Schirmerite	$PbAgBi_3S_6$ to $Pb_3Ag_{1.5}Bi_{3.5}S_9$	disordered						
Andorite VI	$PbAgSb_3S_6$	$^{4,4}L$	*a*13.00	*b*19.15	*c*4.29	–	*Bbmm*	

(Makovicky and Karup-Møller, 1977*b*) has been taken as evidence for this stacking disorder. The 'mineral' schirmerite $PbAgBi_3S_6$–$Pb_3Ag_{1.5}Bi_{3.5}S_9$ is considered as a disordered intergrowth of ^{4}L and ^{7}L homologues (Makovicky and Karup-Møller 1977*b*). Skowron and Tilley (1990), from their HRTEM studies on synthetic material, reported a number of additional homologues, including ^{4,5}L, ^{7,8}L and ^{8,8}L, not known in nature. In addition, they noted a series of longer sequence homologues such as ^{7,4,4}L, ^{7,4,4,4}L and ^{7,4,4,4,4}L and regions of stacking disorder or disordered intergrowth. Their studies indicated that lower temperatures favour a wider variety of homologues, longer ordered sequences and more extensive disorder.

Experimental

A specimen from the gustavite-cosalite-galena paragenesis from the Ivigtut cryolite deposit, Ivigtut, South Greenland, was obtained from the Geological Museum, University of Copenhagen (No. 1973 244). A double-sided polished thin section was prepared using a thermal adhesive and after examination by reflected light microscopy, several areas rich in 'lillianites' were selected. Copper support rings were glued to the surface and the section was heated gently to free the 'lillianite' discs. The discs were Ar ion-milled from both sides until a small hole appeared in the centre of the disc. The ion milled samples were examined in a specially modified JEOL 200CX transmission electron microscope with C_s = 0.41 mm, C_c = 0.91 mm. The theoretical point-to-point resolution for this microscope was 1.8 Å. A series of image simulations was performed by the conventional multi-slice method, using local programs based on the routines by G.R. Anstis and T.B. Williams (pers. comm.) in order to establish the criteria for image interpretation.

Results

Skowron and Tilley (1990) have established the basis for interpretation of images and electron diffraction patterns of the lillianite homologous series. For well ordered regions, the identification of the lillianite homologue is possible using an electron diffraction pattern down the 4 Å zone. The last strong subcell reflection on the 0*k*0 row (00*l* row for monoclinic) corresponds to the 311_{PbS} subcell reflection and the homologue number $N1+N2 = k-4$ ($l-4$). This is illustrated in Fig. 2, which shows a [010] electron diffraction pattern for a well ordered vikingite crystal; the strong subcell reflection 0.0.15 corresponding to 311_{PbS} is indicated. The zigzag nature of the chemical twinned structure is clear in this image

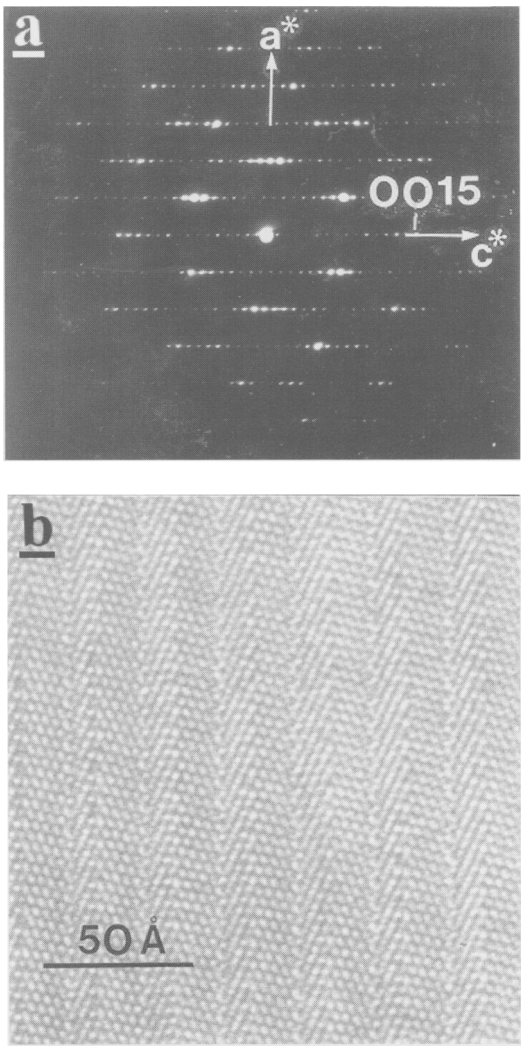

FIG. 2. Electron diffraction pattern and image of a well-ordered vikingite crystal down the [010] zone. (*a*) Electron diffraction pattern. The distribution of intensity along the 00*l* row permits calculation of the homologue number. The last strong subcell reflection along this row corresponds to the $(311)_{PbS}$ subcell and the *l* index of this reflection is related to the homologue number $l-4 = N1+N2$. (*b*) HRTEM image showing the chemically twinned nature of the structure.

(Fig. 2). Figure 3 shows a series of vikingite [010] image simulations for a range of thickness and defocus values. The zigzag nature of the structure becomes less clear as crystal thickness increases or if there is any slight tilting or misalignment of the electron beam or crystal. Skowron and Tilley (1990) noted that the alternating galena-like units usually appear as light and dark bands due to some degree of diffraction contrast from small amounts of beam or crystal tilt. In thick crystals (>100 Å) it is, therefore, generally not possible to distinguish the homologue number of the individual slabs from a HRTEM image but the width of pairs of slabs is easily seen due to diffraction contrast. Thus, in this study it was easy to distinguish from each other 4,4 slabs and 7,4 slabs and also these from $N1 + N2 = 14$ slabs, but it was not possible to establish, unequivocally whether these slabs were 7,7 (heyrovskyite) or 5,9 (eskimoite) units. However, image detail and the structure of crystal defects indicate the slabs are 7,7 rather than 5,9 units.

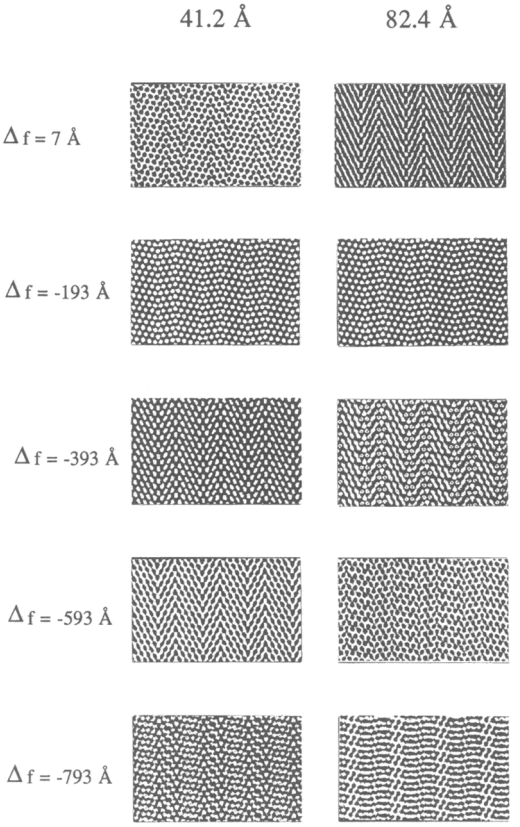

FIG. 3. Series of image simulations for vikingite down the [010] zone.

Block width disorder

In addition to the sharp unstreaked diffraction patterns and well ordered images of the kind shown in Fig. 2, extensive regions of disorder were also observed. A typical diffraction pattern from a comparatively large area of a crystal is shown in Fig. 4*a*. Note both the streaking along c^* and the monoclinic distribution of intensity amongst the subcell reflections. The corresponding image (Fig. 4*b*) shows a disordered intergrowth of ribbons $N = 4$ and $N = 7$ ribbons. Note that the sequences 4,4 (corresponding to gustavite) and 7,4 (vikingite) are by far the most common, a finding in keeping with the inherent stability of the $N = 4$ and $N = 7$ ribbons (Skowron and Tilley, 1990; Makovicky and Karup-Møller, 1977*b* and Karup-Møller, 1977). Crystal chemical data on the $L = 4$ and $L = 7$ slabs by Makovicky *et al.* (1992) indicated that they are electrically neutral and their intergrowth does not involve equilibration of their partial charges by means of regular alternation. The $N1 + N2 = 14$ units (corresponding to heyrovskyite or eskimoite) which are also electrically neutral but reflect a more Pb rich composition, are much less common in the image. It has previously been noted that heyrovskyite is absent as a discrete phase at Ivigtut, (Makovicky and Karup-Møller, 1977*b* and Karup-Møller, 1977) and instead eskimoite (the ^{5,9}L dimorph of heyrovskyite) occurs, although there is no direct evidence for $L = 9$ or $L = 5$ slabs in the sample examined here.

In Fig. 4*b* the longest ordered sequence of slabs is 8 vikingite units 7,4 ($N1 + N2 = 11$). The average value for the region of the crystal shown in Fig. 4*b* is $\mathbf{N} = 4.92$, indicating that it is compositionally intermediate between gustavite ($\mathbf{N} = 4$) and vikingite ($\mathbf{N} = 5.5$). From the average $\mathbf{N}$ value it is possible to calculate, in general terms, the average formula for a region of crystal. However, due to the coupled substitution $2Pb = Ag + Bi$, it is not possible to calculate the actual composition. The composition is $Pb_{3.92-2x}Bi_{2+x}Ag_xS_{6.92}$ and the amount of Ag + Bi for 2 Pb substitution in vikingite and gustavite at Ivigtut is $x \approx 1.2$ (Makovicky and Karup-Møller, 1977*b*).

Detailed examination of the sequence of slabs in Fig. 4*b* reveals some evidence of partial

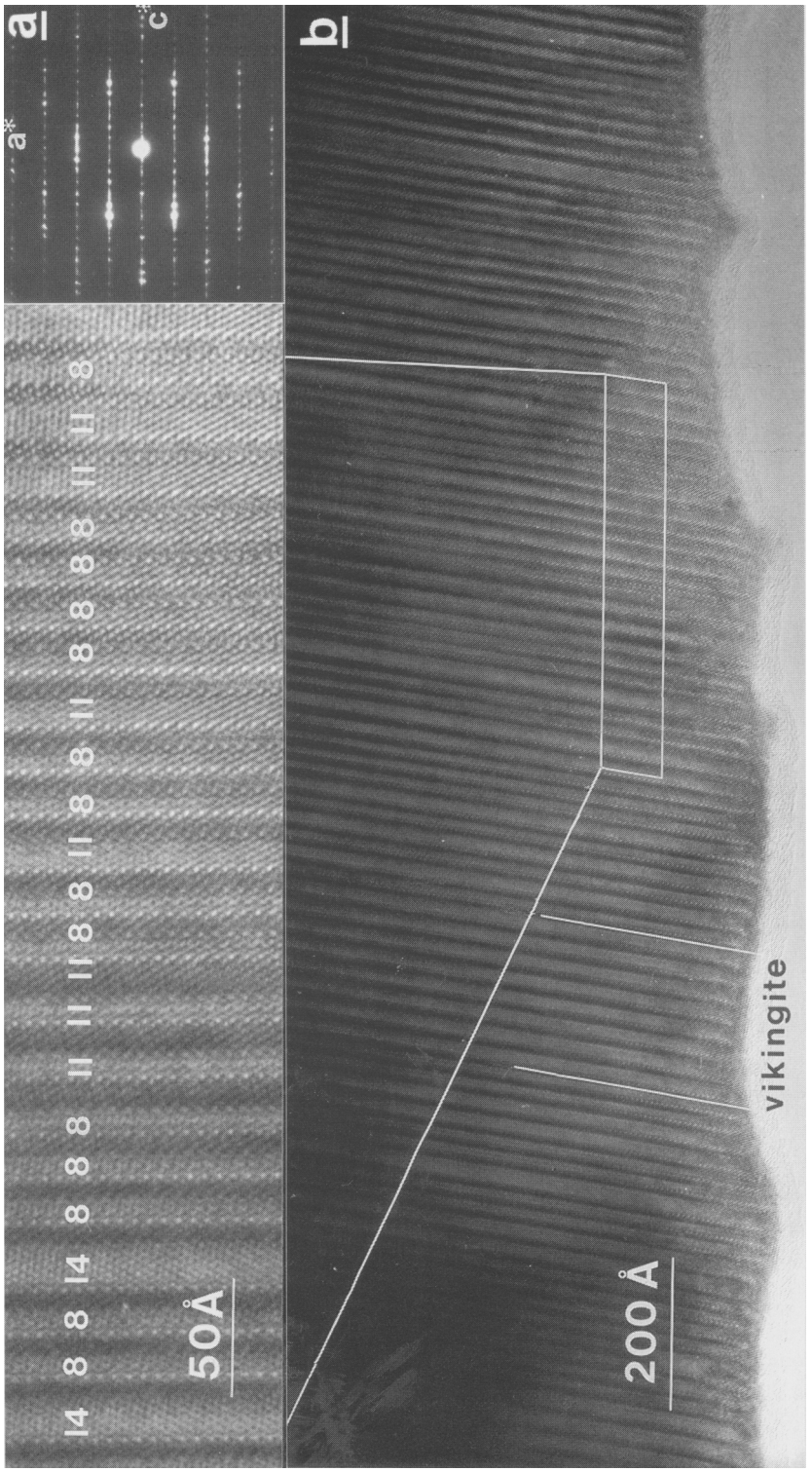

FIG. 4. (*a*) Electron diffraction pattern and image for a disordered intergrowth of gustavite-vikingite and heyrovskyite down the vikingite [010]. Note the streaking of reflections along c^*. (*b*) Image showing the disordered intergrowth of ^{4,4}L, ^{4,7}L and ^{7,7}L blocks (denoted as *N*1 · *N*2 sums). From the weighted average of homologue numbers for the images it is possible to calculate the composition of the disordered area(s), $Pb_{3.92-2x}Bi_{2+x}Ag_xS_{6.92}$ where $\mathbf{N}_{aver} = 4.92$ and $x \approx 1.2$ taken from Makovicky and Karup-Møller (1977*b*).

ordering. There are 163 slabs in the image; 113 $N = 4$ ribbons and 50 $N = 7$ ribbons. The sequence 7,4,4,4 or 4,4,4,7 occurs 20 times in the image, including a section where the sequence is repeated 4 times. The 'heyrovskyite' units generally only occur in single strips although there is a sequence of three such units on the left-hand side of Fig. 4*b*. The sequence 4,4,7,7 occurs eight times in the image while the alternative 7,4,7,7 occurs only twice. The sequence 4,4,7,7 is compositionally equivalent to vikingite, whereas the 7,4,7,7 sequence represents a composition richer in Pb.

Crystal defects

Figure 5 shows HRTEM images of two different crystal defects in which the chemical twin plane $(311)_{PbS}$ is replaced locally by (100) and $(111)_{PbS}$ (or 'jogged') to accommodate change in block width. In both images the crystals are relatively thick and image detail is dominated by diffraction contrast. In Fig. 5*a* a heyrovskyite unit and a gustavite unit change to a pair of vikingite units via a jog of three MS_6 octahedra in the twin plane. Skowron and Tilley (1986) reported similar defects. A more complex defect is shown in Fig. 5b. In this case the unit sequence 4,**7,4,7,7,7, 4,4,4,4,**7,4 is transformed by the jogging of three twin planes to give the sequence, 4,7,**4,4,7,4,7,4,7,4,**7,4. In both of these defects the number of twin planes is conserved in the defect and thus the average value of N (and hence the composition) does not change across the defect.

Discussion

What does this apparently 'pathological disorder' in the 'gustavite/vikingite' crystal represent? In the biopyribole and humite systems, this type of disorder seems to represent trapped compositional and structural intermediates in metasomatic reactions (Veblen and Buseck 1979, White and Hyde, 1982*a*,*b*). In the lillianite system, however, and in sulphides in general, significant atomic diffusion persists at much lower temperatures and this explanation competes with that of a primary or exsolution-produced long-range chemical modulation ('compositional waves') within the

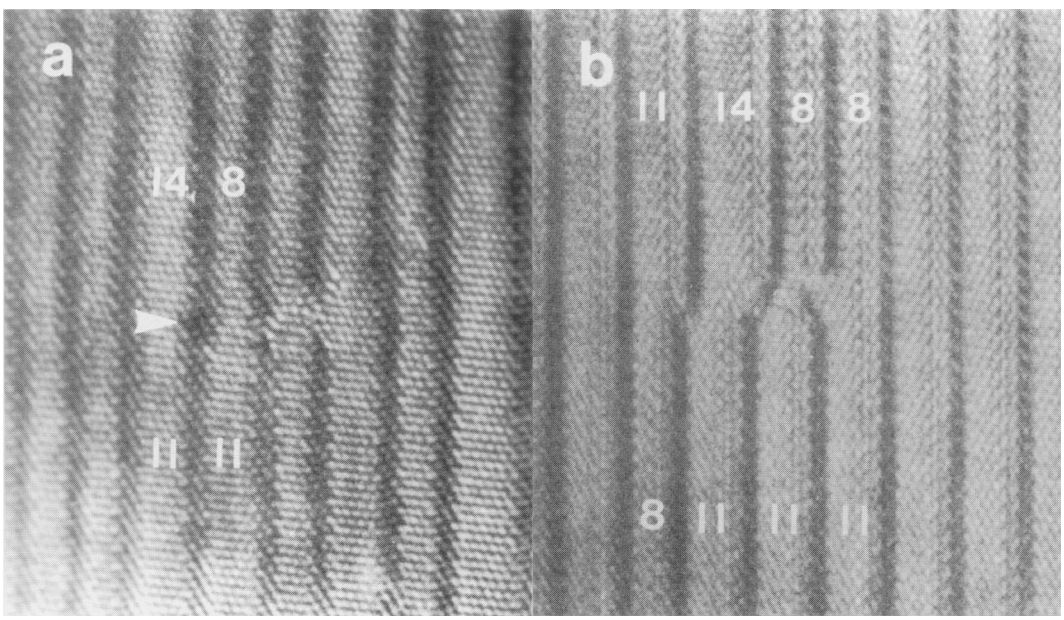

FIG. 5. HRTEM images of two different crystal defects in which the chemical twin plan is altered (or jogged) to accommodate change in block width. (*a*) The sequence **7,7,4,4** is transformed to **7,4,7,4** via a jog of three MS_6 octahedra in the twin plane. (*b*) The sequence **4,7,7,7 4,4,4,4** is transformed by the 'jogging' of three twin planes to give the sequence, **4,4,7,4 7,4,7,4**.

crystal. In order to establish this, one needs to follow the value of **N** across a region of disorder. We employed the simple Axial Next-Nearest Neighbour Ising (ANNNI) model (Price and Yeomans, 1986), where the stacking sequence is treated as the product of competing interactions between first and second nearest neighbour. Using this model the average block-width (as a proxy for the cation variations) was calculated by averaging **N** for each ribbon with the two on either side. The fluctuation of **N** across the crystal region shown in Fig. 4 is presented graphically in Fig. 6, where **N** is plotted against distance across the image in Å from the left-hand edge. A somewhat noisy, step-like variation of average block width (and hence composition) across the crystal can be seen. The compositional fluctuations are of the order of 70–170 Å over the 1800 Å wide region of the crystal, with a 202 Å lamella of ordered vikingite in the central portions. Although the extent of the coupled substitution, Ag + Bi = 2Pb, in the 4 and 7 ribbons, is not known for this disordered crystal fragment, it is fairly constant (67–75%) in individual lillianite homologues from Ivigtut (Makovicky and Karup-Møller, 1984). The variation in **N** across the crystal primarily represents fluctuations in the Pb:Bi ratio rather than Pb:Bi +Ag. Higher **N** values equate to Pb-rich compositions.

Veblen and Buseck (1979) reported a number of long sequence polysomes in their biopyriboles from Chester and noted that many of these long sequence polysomes were polymorphs of the main ordered minerals. They concluded that this indicated that the long sequence polysomes arose not because their free energies were lower than other arrangements of chains, but rather as the result of some growth or reaction mechanism. Veblen and Buseck (1979) noted a chemically logical arrangement of phases on the macroscopic scale (a sequence of minerals is reminiscent of metasomatic zoning on a fine scale), but on the scale observable with HRTEM there was much less regularity in the spatial distribution of ordered and disordered material. Such disorder implies significant and irregular chemical fluctuations over short distances. This type of behaviour is commonly observed in systems that are undergoing diffusion-controlled reactions.

Skowron and Tilley (1990) found that vikingite and lillianite (gustavite) seem to occur over wide areas in the compositional diagram at 773 K. They found disordered intergrowths of 7 and 4 units in the compositional area between lillianite and vikingite (only 4 and 7 units; no 5, 8, 9 or 11). They also noted that the formation of the 4,4 polysome was enhanced at higher temperatures. In addition to the short sequence polysomes they also reported additional 7,4,4, 7,4,4,4, and 7,4,4,4,4 polysomes. Short ordered sequences of the type 7,4,4,4, were also noted in the present study.

In order to evaluate ordering trends in the randomness of the gustavite-vikingite intergrowth

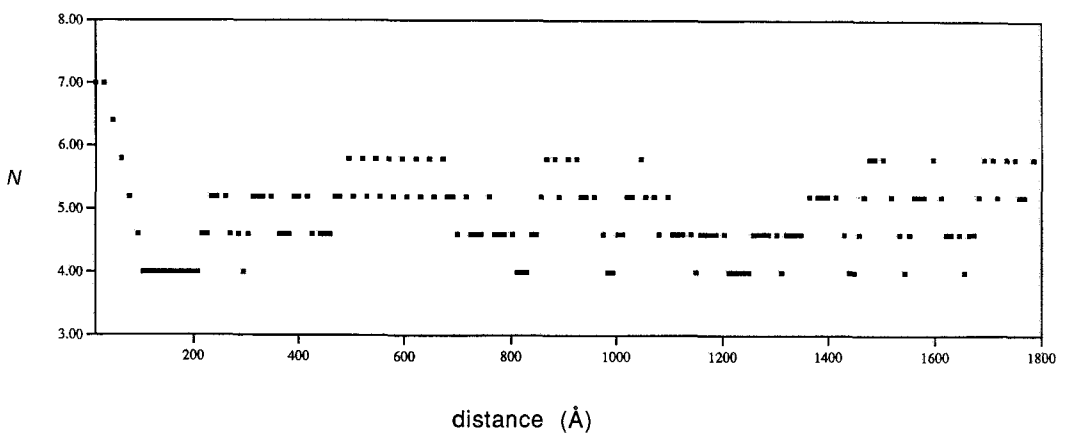

FIG. 6. Schematic representation of block size variation across the crystal region shown in Fig. 4. The block width has been smoothened by using an Axial Next–Nearest Neighbour Ising model, where the width of each block is averaged with its two neighbours on either side. This gave a step-like variation of composition across the large area of crystal shown in Fig. 4.

TABLE 2. Frequency table for pairs, triples and quadruples of slabs in the intergrowth in Fig. 4

Group	Slab combinations and their frequencies				
Pair	4,4 44.3%		4,7* 49.3%		7,7 6.4%
Triple	4,4,4 30.7%	4,4,7* 46.4%		4,7,7* 22.2%	7,7,7 0.7%
Quadruple	4,4,4,4 20.1%	4,4,4,7* 38.9%	4,4,7,7* 38.1%	4,7,7,7* 2.9%	7,7,7,7 0.0%

* Including permutations. Permutations preserve the adjacency conditions (the pairing and the antipathy of identical slabs, respectively) specified by the symbols used.

** Here the combinations 4,4,7,7 and permutations are 18.0%, whereas 4,7,4,7 and permutations are 20.1%.

of slabs, the frequencies of occurrence for all types of layer pairs, triples and quadruples (e.g. 4,4; 4,4,7; 4,4,4,7 etc) were calculated, using a similar approach to that used for mixed-layer silicates (Drits and Sakharov, 1976). All pairs, triples or quadruples in the structure were counted, i.e. we worked with a sliding origin.

For the 140 slabs in the randomly ordered central portion of Fig. 4b, the frequencies of the various sequences are given in Table 2. They show that the dominating slab sequences are 4,4,4,7 and 4,4,7,7, in agreement with the overall chemical $\mathbf{N} = 4.92$, the 4,7,7,7 areas being insignificant and 7,7,7,7 absent. The 4,4,7,7 category is about equally divided into the vikingite sequences 4,7,4,7 and 'anti-vikingite' sequences 4,4,7,7,4,4; these sequences are mostly 2–4 slab pairs thick and separated by 4,4,4,4 sequences with an occasional 7 slab interspersed. Except for a triple sequence of 7,4,4,4 all other $7,4^n$ ($3 \leqslant n \leqslant 9$) sequences are non-periodic. The local 4:7 ratios yielded the configurations in Fig. 6.

The ordered long sequences are not, in general, polymorphs of known minerals but rather compositional intermediates in the series. An exception being the sequence 4,4,7,7 which is a polymorph of vikingite. Vikingite occurs in macroscopically well ordered states, so it is clear that it is more stable than a random intergrowth of 4 and 7 ribbons having the same bulk composition. Similarly, one can argue that the ordered long sequences 7,4,4,4, are also more stable than a random intergrowth of 4 and 7 ribbons having the same bulk composition, but probably less stable than exsolution of vikingite and gustavite. The stability of the observed 4,4,7,7,4,4 sequence and the role of potential screw dislocations for such cases remain unresolved. The long period ordered intergrowths documented here probably represent an intermediate stage in a diffusion controlled exsolution process from a not quite homogeneous, unknown precursor with $\mathbf{N}_{aver} \approx 5$. This concept is in full agreement with the observed structural faults.

In this preliminary study it has not been possible to observe the spatial relationship between ordered and disordered material on the HRTEM scale. More extensive TEM imaging studies, in which the compositional variation will be monitored over much larger distances, are in preparation. It is clear, however, from these preliminary studies that stacking disorder may be rather common in the 'lillianite' minerals at Ivigtut and that this stacking disorder provides a mechanism for compositional variation on a scale of 10s of unit cells.

Acknowledgements

We thank Dr D.A. Jefferson of the Department of Chemistry, University of Cambridge for access to HRTEM facilities, Dr Ole Petersen for the sample and Mr G. Horr for assistance in preparation of the ion thinned specimens. Thanks are also due to Mr B. McHenry, of the South Australian Museum for his help in calculating the stacking sequence for the ANNNI model. The financial support of the Australian Research Council is gratefully acknowledged.

References

Drits, V.A. and Sakharov, B.A. (1976) *X-ray Structure Analysis of Mixed-Layer Minerals. Nauka, Moscow*, (in Russian).

Hoda, S.N. and Chang, L.L. (1975) Phase relations in the system $PbS-Ag_2S-Sb_2S_3$ and $PbS-Ag_2S-Bi_2S_3$. *Amer. Mineral.*, **60**, 621–33.

Karup-Møller, S. (1977) Mineralogy of some Ag–(Cu)–Pb–Bi sulphide associations. *Bull. Geol. Soc. Denmark*, **26**, 41–68.

Makovicky, E. (1977) Chemistry and crystallography of the lillianite homologous series. Part III. Crystal chemistry of the lillianite homologous series. Related phases. *Neues Jahrb. Mineral. Abh.*, **131**, 187–207.

Makovicky, E. (1981) The building principles and classification of bismuth-lead sulphosalts and related compounds. *Fortsch. Mineral.*, **59**, 137–90.

Makovicky, E. (1985) The building principles and classification of sulphosalts based on the SnS archetype. *Fortsch. Mineral.*, **63**, 45–89.

Makovicky, E. (1989) Modular classification of sulphosalts-current status: Definition and application of homologous series. *Neues Jahrb. Mineral. Abh.*, **160**, 269–97.

Makovicky, E. and Karup-Møller, S. (1977*a*) Chemistry and crystallography of the lillianite homologous series. Part I. General properties and definitions. *Neues Jahrb. Mineral. Abh.*, **130**, 264–87.

Makovicky, E. and Karup-Møller, S. (1977*b*) Chemistry and crystallography of the lillianite homologous series. Part II. Definition of new minerals; eskimoite, vikingite, ourayite and treasurite. Redefinition of schirmerite and new data on the lillianite-gustavite solid solution series. *Neues Jahrb. Mineral. Abh.*, **131**, 56–82.

Makovicky E. and Karup-Møller, S. (1984) Ourayite from Ivigtut, Greenland. *Canad. Mineral.*, **22**, 565–75.

Makovicky, E., Mumme, W.G. and Madsen, I.C. (1992) The crystal structure of vikingite. *Neues Jahrb. Mineral. Mh.*, 454–68.

Price, G.D. and Yeomans, J. (1986) A model for polysomatism. *Mineral. Mag.*, **50**, 149–56.

Pring, A. (1989) Structural disorder in aikinite and krupkaite. *Amer. Mineral.*, **74**, 250–5.

Pring, A. (1995) Annealing of synthetic hammarite, $Cu_2Pb_2Bi_4S_9$, and the nature of cation ordering processes in the bismuthinite-aikinite series. *Amer. Mineral.*, **80**, 1168–75.

Skowron, A. and Tilley, R.J.D. (1986) The transformation of chemically twinned phases in the $PbS-Bi_2S_3$ system to the galena structure. *Chemica Scripta*, **26**, 353–8.

Skowron, A. and Tilley, R.J.D. (1990) Chemical twinned phases in the $Ag_2S-PbS-Bi_2S_3$ system. Part 1 Electron microscope study. *J. Solid State Chem.*, **85**, 235–50.

Tilley, R.J.D. and Wright, A.C. (1982) Chemical twinning in the PbS region of the $PbS-Bi_2S_3$ system. *Chemica Scripta*, **19**, 18–22.

Veblen, D.R. and Buseck, P.R. (1979) Chain-width order and disorder in biopyriboles. *Amer. Mineral.*, **64**, 687–700.

Veblen, D.R., Buseck, P.R. and Burnham, C.W. (1977) Asbestiform chain silicates: New minerals and structural groups. *Science*, **198**, 359–63.

White, T.J. and Hyde, B.G. (1982*a*) An electron microscope study of the humite minerals: I Mg-humites. *Phys. Chem. Min.*, **8**, 55–63.

White, T.J. and Hyde, B.G. (1982*b*) An electron microscope study of the humite minerals: II Mn-humites. *Phys. Chem. Min.*, **8**, 167–74.

[*Manuscript received 12 October 1998: revised 19 April 1999*]